Frequency Domain Identification of Multi-Input, Multi-Output Systems Considering Physical Relationships between Measured Variables

Saang Bum Kim[1]; B. F. Spencer Jr., M.ASCE[2]; and Chung-Bang Yun, M.ASCE[3]

Abstract: This paper presents a new frequency domain identification method for multi-input, multi-output (MIMO) systems. Based on experimentally determined frequency response function data, rational polynomial transfer function models of structural systems are identified. Known physical relationships between the measured variables are incorporated in this MIMO frequency domain identification method. The method has three stages: (1) an initial estimation model is generated using a linear least-squares method, (2) the Steiglitz–McBride method is applied to improve the initial estimation model, and (3) a maximum likelihood estimator is optimized using the Levenberg–Marquardt method. For verification of the method, two experimental studies are conducted using shaking table tests; one is the system identification of a smart base-isolated structure employing a magnetorheological (MR) damper, and the other is for an actively controlled two-story, bench-scale building employing an active mass driver. Using the developed method, system models of the experimental structures are estimated, and simulated time histories for the models are compared with measured responses. These comparisons demonstrate that the proposed method is quite effective and robust for system identification of MIMO systems. A graphic user interface program, named *MFDID*, has been developed to realize the suggested method.

DOI: 10.1061/(ASCE)0733-9399(2005)131:5(461)

CE Database subject headings: Identification; Transfer functions; Shake table tests; Vibration control; Frequency.

Introduction

The goal of system identification is to build accurate, simplified models based on observed input/output data (Ljung 1999), allowing for the investigation of system characteristics from experimental data. Many researchers have applied system identification techniques to large civil infrastructure systems for health monitoring, damage detection, and vibration control (Yun and Shinozuka 1980; Dyke et al. 1994). For system identification of linear time invariant systems from stationary responses with a sufficiently large amount of data, frequency domain identification methods can be used to obtain accurate and precise models. In the frequency domain methods, transfer function models are obtained from measured data by minimizing some measure of the error between the model and measurements (Levy 1959; Smith 1983; Ewins 1991; Hong and Yun 1993; Juang 1994; Pintelon et al. 1994; Barford 1997; de Vries and Van den Hof 1998; McCormack and Godfrey 1998; Anthonis et al. 1999).

For identification of dynamic models of structural systems, absolute accelerations are usually measured, due to their ease of measurement and cost effectiveness. However, system models identified from measured acceleration responses may generate biased results in the low-frequency range, particularly when these models are used to estimate relative displacement or relative velocity responses. These responses often contain important information for the design of structural control systems. Balmès (1996) developed a frequency domain identification method, which can consider the minimality and reciprocity of the structural systems. Jin et al. (2000) suggested a frequency domain identification method, which can consider fixed zeros and poles, and applied it to a structural system controlled by two active mass drivers (AMDs). However, the performance of these methods depends on the choice of weighting function.

In this research, the system is modeled as a rational polynomial transfer function, where the modeling error is assumed a Gaussian white noise. Constraints of the transfer function's coefficient matrices are derived from the physical relationships between the measured input and output quantities. These constraints are incorporated in the frequency domain identification strategy to prevent biased or unstable identification. A rational polynomial model of the transfer function is estimated by the maximum likelihood estimator (Pintelon et al. 1994), which is strongly consistent and asymptotically efficient (Kumar and Varaiya 1986; Chae 2000). This estimation problem takes the form of a nonlinear least-squares problem. To solve the nonlinear optimization problem in a more effective and robust way, a three-stage procedure is suggested. In the first stage, an initial estimation model is obtained using the linear least squares-method, and then the estima-

[1]Research Engineer, Civil Structure Part, Technology Division, Samsung Corporation, 4th Fl., Seohyun Bldg., 270-1, Bundang-Gu, Sungnam-Si, Gyonggi-Do, 463-824 Republic of Korea.

[2]Nathan M. and Anne M. Newmark Endowed Chair of Civil Engineering, Dept. of Civil and Environmental Engineering, Univ. of Illinois at Urbana and Champaign, 2213 Newmark Civil Engineering Laboratory, MC-250, 205 North Matthews Ave., Urbana, IL 61801. E-mail: bfs@uiuc.edu

[3]Professor, Civil Engineering, Korea Advanced Institute of Science and Technology, 373-1, Kusong-dong, Yusong-gu, Taejon-si, 305-701 Republic of Korea. E-mail: ycb@kaist.ac.kr

Note. Discussion open until October 1, 2005. Separate discussions must be submitted for individual papers. To extend the closing date by one month, a written request must be filed with the ASCE Managing Editor. The manuscript for this paper was submitted for review and possible publication on September 11, 2003; approved on May 3, 2004. This paper is part of the ***Journal of Engineering Mechanics***, Vol. 131, No. 5, May 1, 2005. ©ASCE, ISSN 0733-9399/2005/5-461–472/$25.00.

tion model is further improved using the Steiglitz–McBride method. Finally, the Levenberg–Marquardt method is applied to obtain the maximum likelihood estimate. Experimental results of shaking table tests are given to demonstrate the efficacy of the proposed approach.

Rational Polynomial Transfer Function Model with Physical Relationships between Measured Variables

The input–output relationship for linear time invariant (LTI) dynamical systems can be modeled by differential equations, and if the effects of the initial conditions are ignored, it can be represented by the rational polynomial transfer function model in the Laplace domain. The rational polynomial representation of the transfer function can be extracted from the experimentally determined frequency response function (FRF) data. The FRF represents the system's input–output behavior at steady state. The coefficients of the denominator polynomials are related to the natural frequencies and damping ratios for the system, and the coefficients of the numerator polynomials are related to the mode shapes of the system. The FRF for an LTI system can be obtained by evaluating the transfer function on the imaginary axis (Levi 1959; Smith 1983; Goodwind and Sin 1984; Ewins 1991; Hong and Yun 1993; Mamum et al. 2002).

The physical relationships between input and output signals frequently dictate certain constraints on the coefficients of the rational polynomial transfer function model. In this paper, the constraints on the transfer function's coefficients are derived for lightly damped structural systems.

Consider a structure with n_s degree-of-freedom excited by a one-dimensional ground acceleration, $\ddot{y}_g(t)$, and external excitation forces, $\mathbf{f}_e(t)$. The equation of motion can be written as follows:

$$\mathbf{M}_s\ddot{\mathbf{y}}_{sr}(t) + \mathbf{C}_s\dot{\mathbf{y}}_{sr}(t) + \mathbf{K}_s\mathbf{y}_{sr}(t) = \mathbf{B}_{se}\mathbf{f}_e(t) - \mathbf{M}_s\mathbf{B}_{sg}\ddot{y}_g(t) \tag{1}$$

where $\mathbf{y}_{sr}(t)$ = relative displacement of structure; $\mathbf{M}_s$, $\mathbf{C}_s$, and $\mathbf{K}_s$ = mass, damping, and stiffness matrices, respectively; and $\mathbf{B}_{se}$ and $\mathbf{B}_{sg}$ = matrices which represent the effects on the structural responses due to the external excitation force and ground acceleration, respectively.

The equation of motion can be rewritten in the state space representation as follows:

$$\dot{\mathbf{x}}(t) = \mathbf{A}\mathbf{x}(t) + \mathbf{B}_f\mathbf{f}_e(t) + \mathbf{B}_g\ddot{y}_g(t) \tag{2}$$

where

$$\mathbf{x}(t) = \begin{bmatrix} \mathbf{y}_{sr}(t) \\ \dot{\mathbf{y}}_{sr}(t) \end{bmatrix}; \quad \mathbf{A} = \begin{bmatrix} \mathbf{0} & \mathbf{I} \\ -\mathbf{M}_s^{-1}\mathbf{K}_s & -\mathbf{M}_s^{-1}\mathbf{C}_s \end{bmatrix}$$

$$\mathbf{B}_f = \begin{bmatrix} \mathbf{0} \\ \mathbf{M}_s^{-1}\mathbf{B}_{se} \end{bmatrix}; \quad \mathbf{B}_g = \begin{bmatrix} \mathbf{0} \\ \mathbf{M}_s^{-1}\mathbf{B}_{sg} \end{bmatrix}$$

From the above equation, transfer functions from the two inputs, $\mathbf{f}_e(t)$ and $\ddot{y}_g(t)$ to the relative displacement can be obtained as follows:

$$\mathbf{H}_{\mathbf{y}_{sr}\mathbf{f}_e}(s) = [\mathbf{I} \quad \mathbf{0}](s\mathbf{I} - \mathbf{A})^{-1}\begin{bmatrix} \mathbf{0} \\ \mathbf{M}_s^{-1}\mathbf{B}_{se} \end{bmatrix} \tag{3}$$

$$\mathbf{H}_{\mathbf{y}_{sr}\ddot{y}_g}(s) = [\mathbf{I} \quad \mathbf{0}](s\mathbf{I} - \mathbf{A})^{-1}\begin{bmatrix} \mathbf{0} \\ -\mathbf{B}_{sg} \end{bmatrix} \tag{4}$$

where $\mathbf{H}_{\mathbf{y}_{sr}\mathbf{f}_e}(s)$ and $\mathbf{H}_{\mathbf{y}_{sr}\ddot{y}_g}(s)$ = transfer function from the external excitation force and from the ground acceleration, respectively, to the relative displacement.

The number of poles for theses systems is $2n_s$, and maximum number of zeros for each element in the transfer function matrices is $2n_s-2$ (see the Appendix), which can be represented as follows:

$$\mathbf{H}_{\mathbf{y}_{sr}\mathbf{f}_e}(s) = \frac{\beta_{0,\mathbf{f}} + \beta_{1,\mathbf{f}}s + \cdots + \beta_{2n_s-2,\mathbf{f}}s^{2n_s-2}}{1 + \alpha_1 s + \cdots + \alpha_{2n_s}s^{2n_s}} \tag{5}$$

$$\mathbf{H}_{\mathbf{y}_{sr}\ddot{y}_g}(s) = \frac{\beta_{0,g} + \beta_{1,g}s + \cdots + \beta_{2n_s-2,g}s^{2n_s-2}}{1 + \alpha_1 s + \cdots + \alpha_{2n_s}s^{2n_s}} \tag{6}$$

where α_k $(k=1,2,\ldots,2n_s)$ = real coefficients of the denominator; $\beta_{k,\mathbf{f}}$ and $\beta_{k,g}$ $(k=0,1,\ldots,2n_s-2)$ = real coefficient matrices for the numerator polynomials for $\mathbf{H}_{\mathbf{y}_{sr}\mathbf{f}_e}(s)$ and $\mathbf{H}_{\mathbf{y}_{sr}\ddot{y}_g}(s)$, respectively.

From the above equations, the transfer functions from the two inputs to the absolute acceleration can be derived as

$$\mathbf{H}_{\ddot{\mathbf{y}}_s\mathbf{f}_e}(s) = s^2\mathbf{H}_{\mathbf{y}_{sr}\mathbf{f}_e}(s) = \frac{\beta_{0,\mathbf{f}}s^2 + \beta_{1,\mathbf{f}}s^3 + \cdots + \beta_{2n_s-3,\mathbf{f}}s^{2n_s-1} + \beta_{2n_s-2,\mathbf{f}}s^{2n_s}}{1 + \alpha_1 s + \cdots + \alpha_{2n_s}s^{2n_s}} \tag{7}$$

or

$$\mathbf{H}_{\ddot{\mathbf{y}}_s\mathbf{f}_e}(s) \triangleq \frac{\mathbf{B}_{0,\mathbf{f}} + \mathbf{B}_{1,\mathbf{f}}s + \cdots + \mathbf{B}_{2n_s-1,\mathbf{f}}s^{2n_s-1} + \mathbf{B}_{2n_s,\mathbf{f}}s^{2n_s}}{1 + \alpha_1 s + \cdots + \alpha_{2n_s}s^{2n_s}} \tag{8}$$

$$\mathbf{H}_{\ddot{\mathbf{y}}_s\ddot{y}_g}(s) = [\mathbf{1}] + s^2\mathbf{H}_{\mathbf{y}_{sr}\ddot{y}_g}(s) = \frac{1 + \alpha_1 s + (\alpha_2 + \beta_{0,g})s^2 + (\alpha_3 + \beta_{1,g})s^3 + \cdots + (\alpha_{2n_s-1} + \beta_{2n_s-3,g})s^{2n_s-1} + (\alpha_{2n_s} + \beta_{2n_s-2,g})s^{2n_s}}{1 + \alpha_1 s + \cdots + \alpha_{2n_s}s^{2n_s}} \tag{9}$$

or

$$\mathbf{H}_{\ddot{\mathbf{y}}_s \ddot{y}_g}(s) \triangleq \frac{\mathbf{B}_{0,g} + \mathbf{B}_{1,g}s + \mathbf{B}_{2,g}s^2 + \mathbf{B}_{3,g}s^3 \cdots + \mathbf{B}_{2n_s-1,g}s^{2n_s-1} + \mathbf{B}_{2n_s,g}s^{2n_s}}{1 + \alpha_1 s + \cdots + \alpha_{2n_s}s^{2n_s}} \tag{10}$$

where $\mathbf{H}_{\ddot{\mathbf{y}}_{sr}\mathbf{f}_e}(s)$ and $\mathbf{H}_{\ddot{\mathbf{y}}_{sr}\ddot{y}_g}(s)$ = transfer functions from the external excitation force and ground acceleration, respectively, to the absolute accelerations; and $\mathbf{B}_{k,\mathbf{f}}$ and $\mathbf{B}_{k,g}$ = real coefficient matrices for the numerator polynomials for $\mathbf{H}_{\ddot{\mathbf{y}}_{sr}\mathbf{f}_e}(s)$ and $\mathbf{H}_{\ddot{\mathbf{y}}_{sr}\ddot{y}_g}(s)$, respectively.

By comparing the coefficient matrices of the transfer function model for the absolute acceleration [Eqs. (8) and (10)] with those derived from the transfer functions of relative displacements [Eqs. (7) and (9)], the following constraint equations can be obtained:

$$\mathbf{B}_{0,\mathbf{f}} = \mathbf{0}, \quad \mathbf{B}_{1,\mathbf{f}} = \mathbf{0} \tag{11}$$

$$\mathbf{B}_{0,g} - 1 = \mathbf{0}, \quad \mathbf{B}_{1,g} - \alpha_1 = \mathbf{0} \tag{12}$$

Using the constraint equations, Eqs. (8) and (10) can be rewritten, respectively, as follows:

$$H_{mn}(s) = \frac{\Phi_{B,mn}(s)\theta_{B,mn}}{1 + \Phi_a(s)\theta_a} = \frac{\Phi_{Bc,mn}(s)\theta_{Bc,mn} + \Phi_{ac,mn}(s)\theta_a}{1 + \Phi_a(s)\theta_a} \tag{13}$$

where $H_{mn}(s)$ = transfer function model of the system from the nth excitation to the mth response; $\theta_{B,mn} = [B_{0,mn}, B_{1,mn}, \ldots, B_{2n_s,mn}]^T$ and $\theta_{Bc,mn} = [B_{2,mn}, B_{3,mn}, \ldots, B_{2n_s,mn}]^T$ = vectors of coefficients for the numerator before and after the constraints have been imposed, respectively; $\theta_a = [a_1, a_2, \ldots, a_{2n_s}]^T$ = vectors of coefficients for the denominator polynomials; $\Phi_{B,mn}(s) = [1, s, \ldots, s^{2n_s}]$ and $\Phi_{Bc,mn}(s) = [s^2, s^3, \ldots, s^{2n_s}]$ = corresponding frequency domain regression matrices for the numerator before and after the constraints have been imposed, respectively; $\Phi_a(s) = [s, s^2, \ldots, s^{2n_s}]$ = corresponding frequency domain regression matrices for the denominator polynomials; $\Phi_{ac,mn}(s) = \Phi_a(s)\mathbf{B}_{ca,mn}$; and $\mathbf{B}_{ca,mn}$ = Boolean matrix, which indicates the effects of physical relationships. In the case of the external excitation force input, $\mathbf{B}_{ca,mn} = \mathbf{0}_{(2n_s)\times(2n_s)}$, and in the case of the ground acceleration input

$$\mathbf{B}_{ca,mn} = \begin{bmatrix} \mathbf{I}_{2\times 2} & \mathbf{0} \\ \mathbf{0} & \mathbf{0}_{(2n_s-2)\times(2n_s-2)} \end{bmatrix}$$

Maximum Likelihood Estimator of Transfer Function Model

Herein, the error between the rational polynomial model and the experimentally determined frequency response function (FRF) is assumed independent and normally distributed at each frequency. These assumptions are asymptotically valid for linear systems under persistent excitation with additive Gaussian white noise measurement errors (Pintelon et al. 1994). By maximizing the likelihood function of the conditional distribution for the experimentally determined FRF, given the unknown system parameter vector, the following maximum likelihood estimator can be obtained (Pintelon et al. 1994).

$$\theta_{\mathrm{ML}} = \arg\min_{\theta} \left(\sum_m \sum_n \sum_l \left| H_{\exp,mn}(\omega_l) - \frac{\Phi_{B,mn}(j\omega_l)\theta_{B,mn}}{1 + \Phi_a(j\omega_l)\theta_a} \right|^2 \Sigma^{-1}_{H_{mn}}(\omega_l) \right) \tag{14}$$

where $j = \sqrt{-1}$; $H_{\exp,mn}(\omega_l)$ = experimentally determined FRF data at the frequency ω_l from the nth excitation to the mth response; and $\Sigma_{H_{mn}}(\omega_l)$ = variance for the experimentally determined FRF data.

To effectively solve the nonlinear optimization problem given in Eq. (14), a three-stage procedure is employed.

Stage I

In the first stage, the nonlinear optimization problem given in Eq. (14) is linearized by multiplying the denominator of the rational polynomial model and the magnitude of the experimentally determined FRF

$$\theta_{\mathrm{LLS}} = \arg\min_{\theta} \sum_m \sum_n \sum_l \left(\left| H_{\exp,mn}(\omega_l)[1 + \Phi_a(j\omega_l)\theta_a] - \Phi_{B,mn}(j\omega_l)\theta_{B,mn} \right|^2 \left| H_{\exp,mn}(\omega_l) \right|^2 \Sigma^{-1}_{H_{mn}}(\omega_l) \right) \tag{15}$$

This linearized problem is then solved by a linear-least squares (LLS) method. Because the error function used here can be assumed as the original error function multiplied by the numerator of the rational polynomial model, the errors are weighted less near the zeros. Recently, importance of the zero dynamics has been emphasized by many researchers (Huang and Youcef-Toumi 1999). To obtain the accurate system model, this undesirable effect should be corrected (Oppenheim et al. 1975; Mamum et al. 2002).

Stage II

To eliminate the problem regarding the weighting of the error function found in the previous stage, the Steiglitz–McBride method is applied. This method is an iterative approach, starting from the LLS solution obtained in the previous stage, given by

$$\theta_{\mathrm{SM}}[k+1] = \arg\min_{\theta} \sum_m \sum_n \sum_l \left(\left| H_{\exp,mn}(\omega_l)[1 + \Phi_a(j\omega_l)\theta_a] - \Phi_{B,mn}(j\omega_l)\theta_{B,mn} \right|^2 \frac{\Sigma^{-1}_{H_{mn}}(\omega_l)}{[1 + \Phi_a(j\omega_l)\theta_a[k]]^2} \right) \tag{16}$$

At each iteration step, the weighting function is updated using the parameters obtained from the previous step, and $\theta_a[k]$ on the right-hand side of Eq. (16) is fixed to get a LLS problem yielding $\theta_{\mathrm{SM}}[k+1]$. This method usually converges rapidly in practice, but convergence is not guaranteed; convergence may not occur if the model order is too large (Ljung 1999).

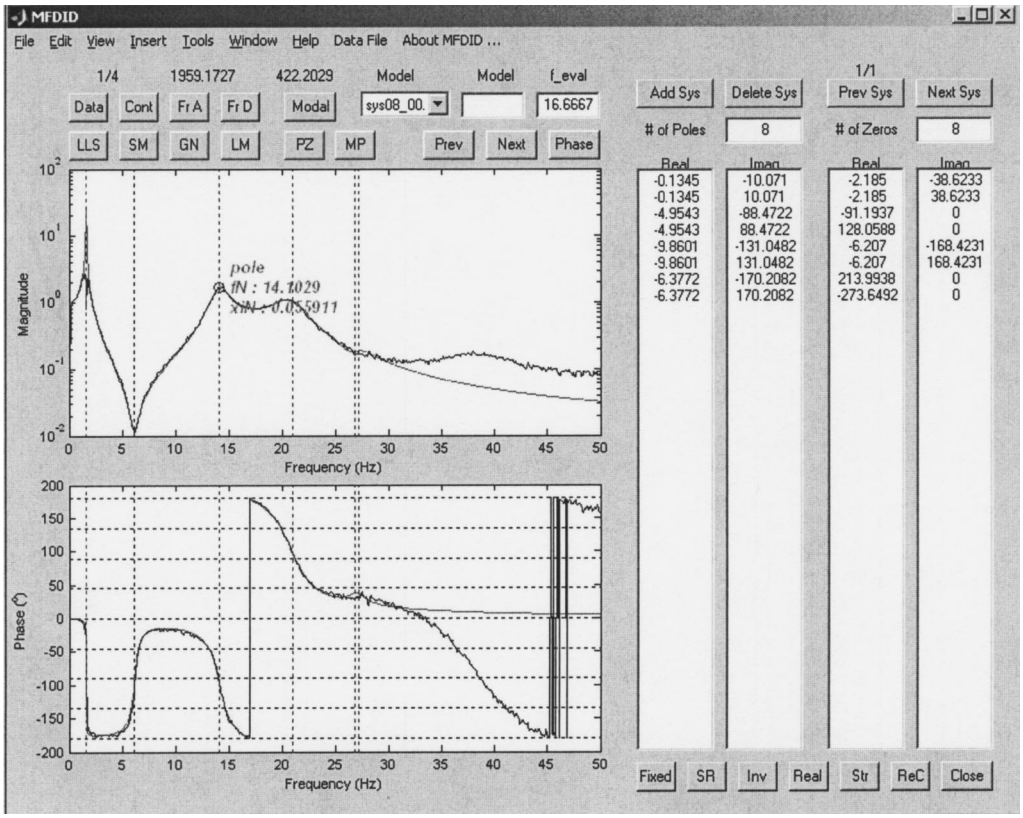

Fig. 1. Screen capture of *MFDID* program

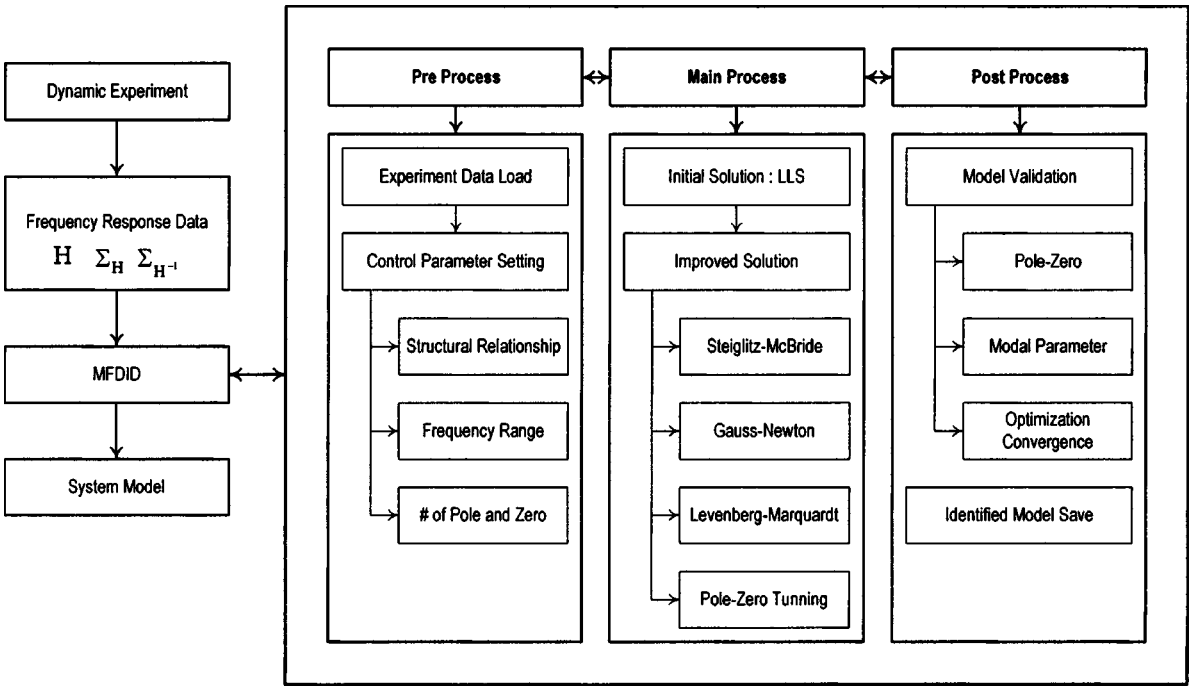

Fig. 2. Flow chart of system identification using *MFDID*

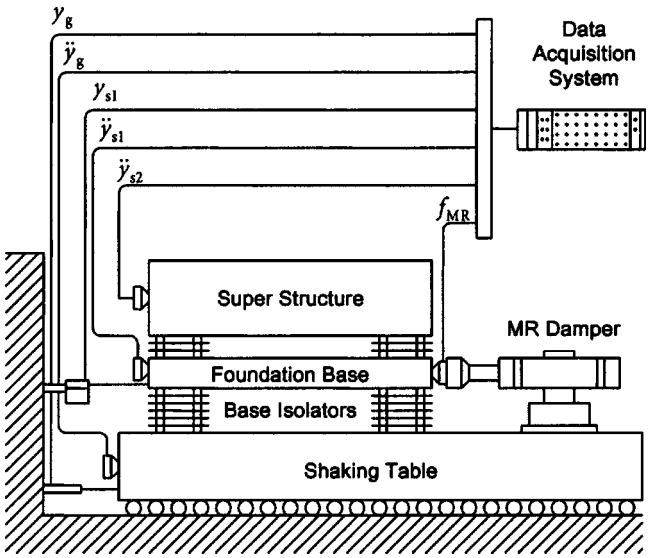

Fig. 3. Experimental setup of shaking table test at University of Notre Dame

Stage III

In the third stage, the final solution is obtained using the Levenberg–Marquardt method, which is a nonlinear optimization method (Dennis and Schnabel 1983; Luenberger 1984). In this stage, the maximum likelihood estimator is approximated as a quadratic polynomial equation using the Taylor series expansion at each iteration step. This quadratic optimization problem is solved with a mixed quadratic and cubic line search procedure, given by

$$\theta_{LM}[k+1] = \theta_{LM}[k] + \Delta\theta_{LM}[k] \tag{17}$$

$$\Delta\theta_{LM}[k] = \underset{\|\Delta\theta\|_2 < \lambda_{LM}[k]}{\arg\min} \sum_m \sum_n \sum_l \left(\left| H_{\exp,mn}(\omega_l) - \frac{\Phi_{B,mn}(j\omega_l)\theta_{B,mn}[k]}{1+\Phi_a(j\omega_l)\theta_a[k]} - \sum_\theta \frac{\partial}{\partial\theta}\left(\frac{\Phi_{Bc,mn}(j\omega_l)\theta_{Bc,mn}[k]}{1+\Phi_a(j\omega_l)\theta_a[k]} \right) \Delta\theta[k] \right|^2_{\Sigma^{-1}_{H_{mn}}} \right) \tag{18}$$

where $\lambda_{LM}[k]$=scalar: step size in the Levenberg–Marquardt method

The method is realized in the *Matlab* environment as the program *MFDID* (see Fig. 1). The procedure for the system identification is summarized in Fig. 2.

Experimental Studies Using Shaking Table Tests

Two examples are considered to demonstrate the efficacy of the proposed approach.

Smart Base-Isolated Structure Employing an Magnetorheological Damper

System identification of a smart base-isolated structure employing an MR damper is considered (see Fig. 3). Shaking table tests were conducted using a hydraulic uniaxial seismic simulator at the University of Notre Dame (Fig. 4). The specifications for this seismic simulator are summarized in Table 1 (Yoshioka et al. 2002).

The smart base-isolated structure consists of two masses; the top mass represents the superstructure, whereas the bottom mass represents the foundation base. An MR damper is installed between the foundation base and the ground to reduce the vibration

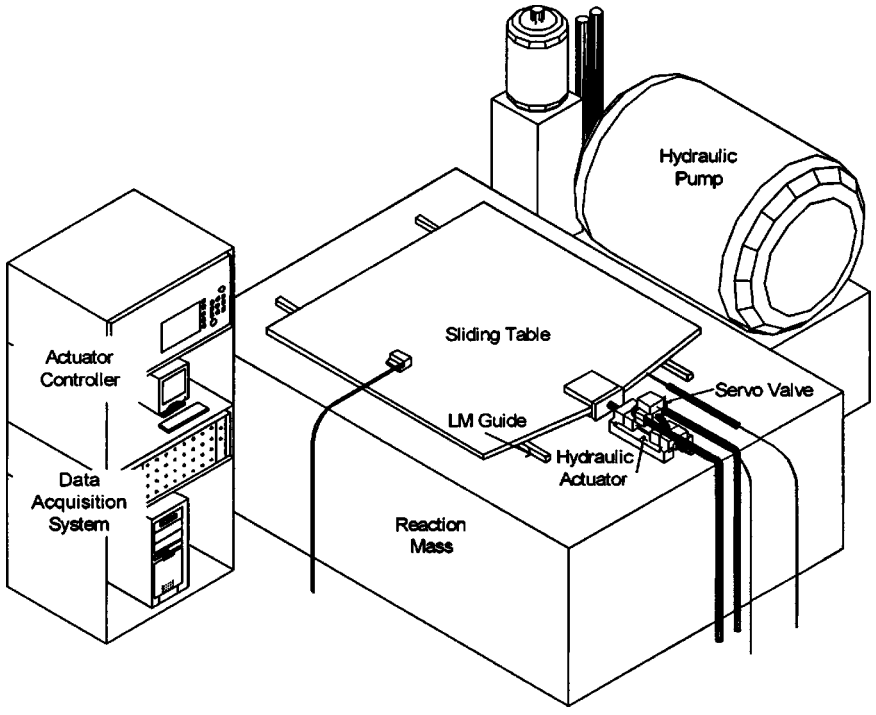

Fig. 4. Hydraulic shaking table at University of Notre Dame

Table 1. Specification of the Seismic Simulator at University of Notre Dame

Aluminum sliding table	122 cm × 122 cm	Maximum displacement	±5 cm
Operational frequency range	0–50 Hz[a]	Maximum velocity	±90 cm/s[a]
Hydraulic power	3.75 kW	Maximum acceleration	±4g[a]

[a]Under the test load: 500 kg.

Table 2. Identified Modal Characteristics of the Smart Base-Isolated Structure

Mode number	First	Second	Third	Fourth
Natural frequency (Hz)	1.6364	14.1064	20.8944	27.1136
Modal damping ratio (%)	2.43	5.44	7.44	3.71

of the superstructure due to the earthquake excitation. Fig. 3 shows a schematic of the test model and its experimental setup.

In this experiment, the system has two inputs, which are the earthquake's ground acceleration and the force of the MR damper. The ground acceleration is generated by the movement of the shaking table. The force of the MR damper is generated according to the commanded current and the movement across the MR damper.

Using the *MFDID* program, a rational polynomial model for the smart base-isolated structure is identified. The frequency ranges below 0.25 Hz and above 32.5 Hz are excluded to eliminate DC error and to prevent the unwanted higher mode effects, respectively. The inverse of the variance of the experimental FRF data are used as a weighting function in Eq. (13) (Fig. 5).

The identified modal parameters are summarized in Table 2. The identified FRF is compared with the experimental FRF data in Fig. 6. The identified model shows good agreement with the experimental FRF data in the frequency range up to 30 Hz.

Fig. 7 shows the identified FRF at each stage. In the first stage, the global trend of the FRF is matched using a linear least-squares method, and in the second stage, using the Steiglitz–McBride method, local trends, especially near the first pole and first nonzero zero, are matched. Finally, in the third stage, the refined rational polynomial model is obtained using the Levenberg–Marquardt method. The convergence of error norm in each iterative optimization process is shown in Fig. 8. Using the *MFDID* program, the poles and zeros of the system models can also be adjusted manually; this manually adjusted model can be used as an initial solution for the iterative method, such as the Steiglitz–McBride method or the Levenberg–Marquardt method.

To investigate the importance of incorporating the physical relationships between the measured variables discussed in "Rational Polynomial Transfer Function Model…," another system model is derived for the smart base-isolated structure without considering these relationships. Fig. 9 shows the comparison of FRFs for two system models; one is optimized without considering the physical relationships, and the other is optimized considering the physical relationships. For the FRFs to absolute accelerations, both models show good agreement with experimental results. However, for the relative displacement FRF, low frequency distortions arise in the model constructed without considering the physical relationships, while the model considering the physical relationships shows stable results.

Numerical simulation using the identified model has been conducted to verify the suggested method. Signals for the external excitation force and the ground acceleration measured from the experiment are applied to the identified system model, and simulation responses for the system model are compared with measured responses of the structure. The signal-to-error ratios $[20\log(\sigma_{\text{Signal}}/\sigma_{\text{Error}})]$ are found to be 4.37 dB for the absolute acceleration of the base structure and 11.64 dB for the absolute acceleration of the superstructure (Fig. 10).

One of the main application areas of the proposed method is development of system models for the structural vibration control. The MR damper is considered as an effective response control

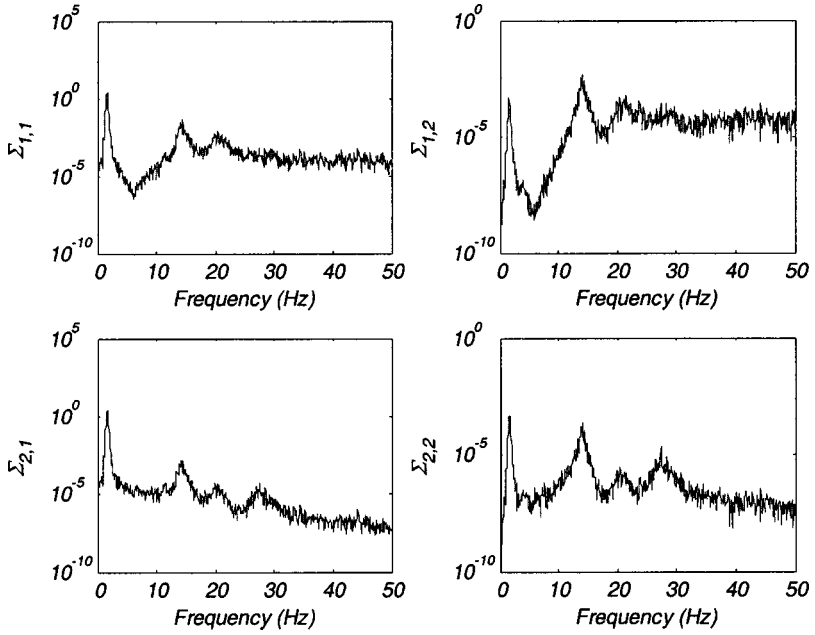

Fig. 5. Variances in the experimentally determined frequency response function data

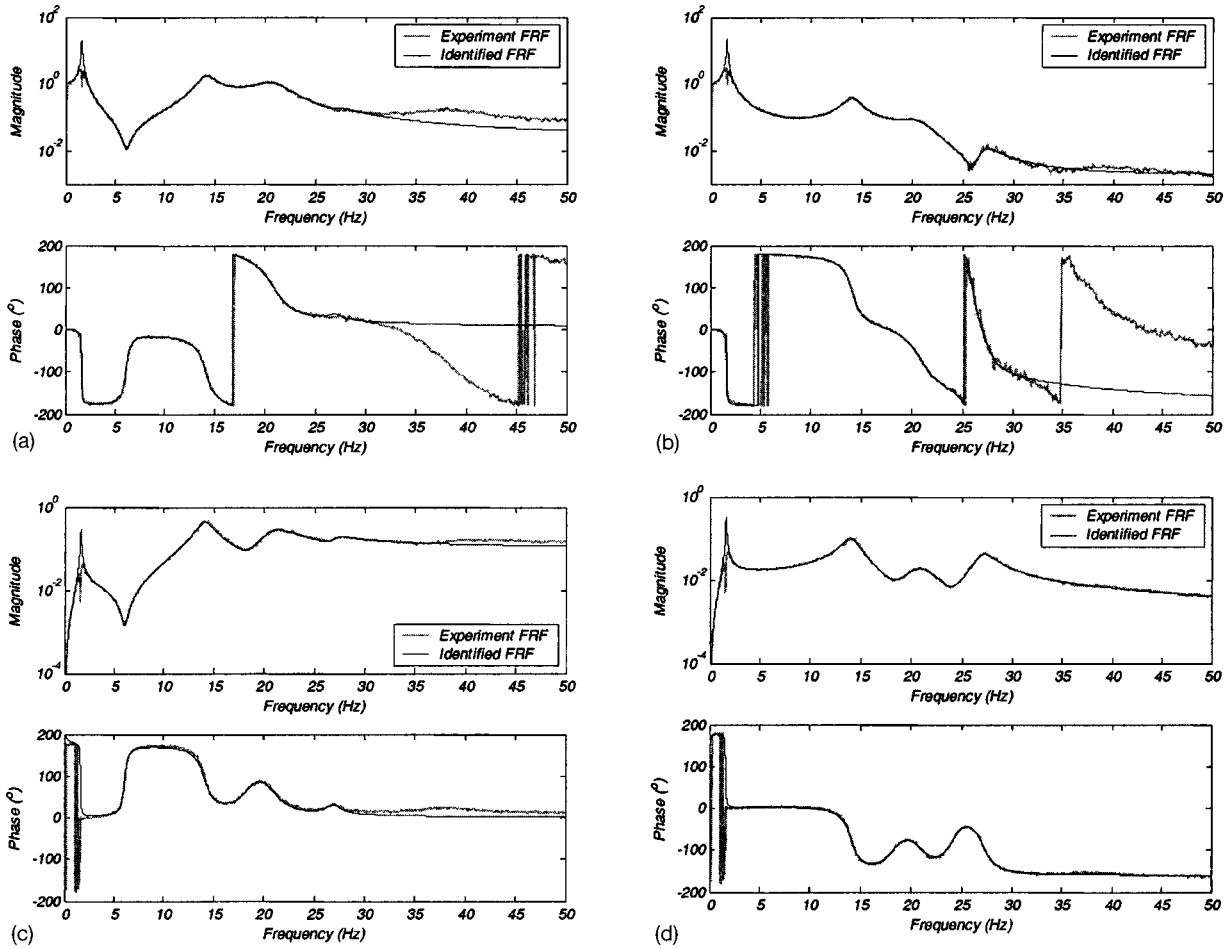

Fig. 6. Identified frequency response functions: (a) frequency response function (FRF) for absolute acceleration of foundation base from ground acceleration; (b) FRF for absolute acceleration of superstructure from ground acceleration; (c) FRF for absolute accelerations of foundation base from magnetorheological (MR) damper force; and (d) FRF for absolute acceleration of superstructure from MR damper force

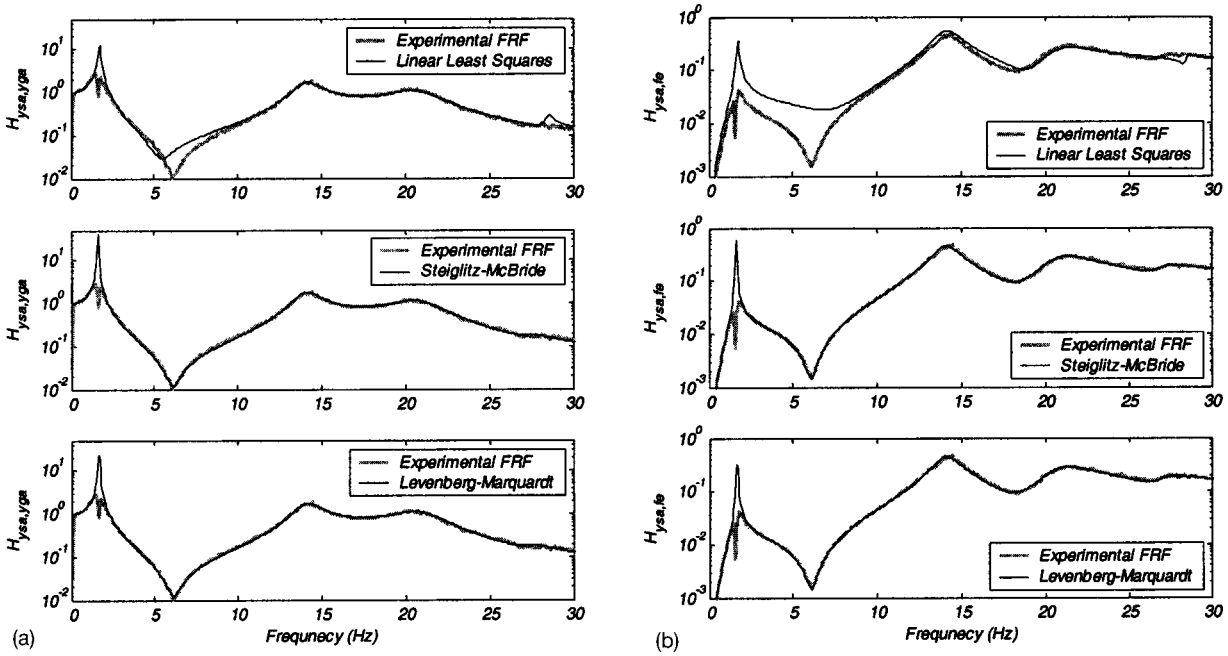

Fig. 7. Identified transfer function along the optimization stages: (a) frequency response function (FRF) for absolute acceleration of foundation base from ground acceleration; and (b) FRF for absolute acceleration of foundation base from magnetorheological damper force

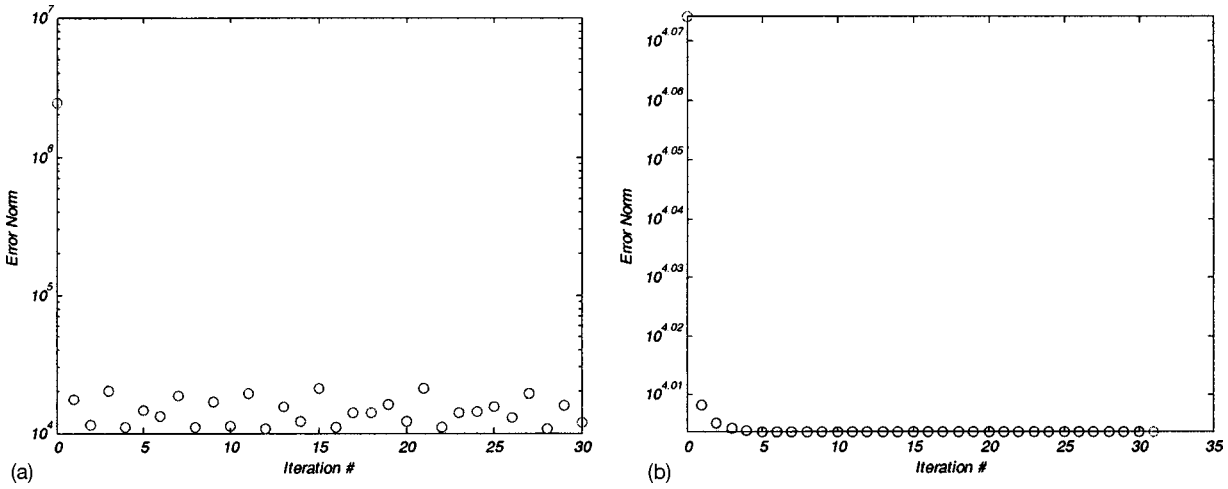

Fig. 8. Convergence of error norm with optimization processes: (a) Steiglitz–McBride method; and (b) Levenberg–Marquardt method

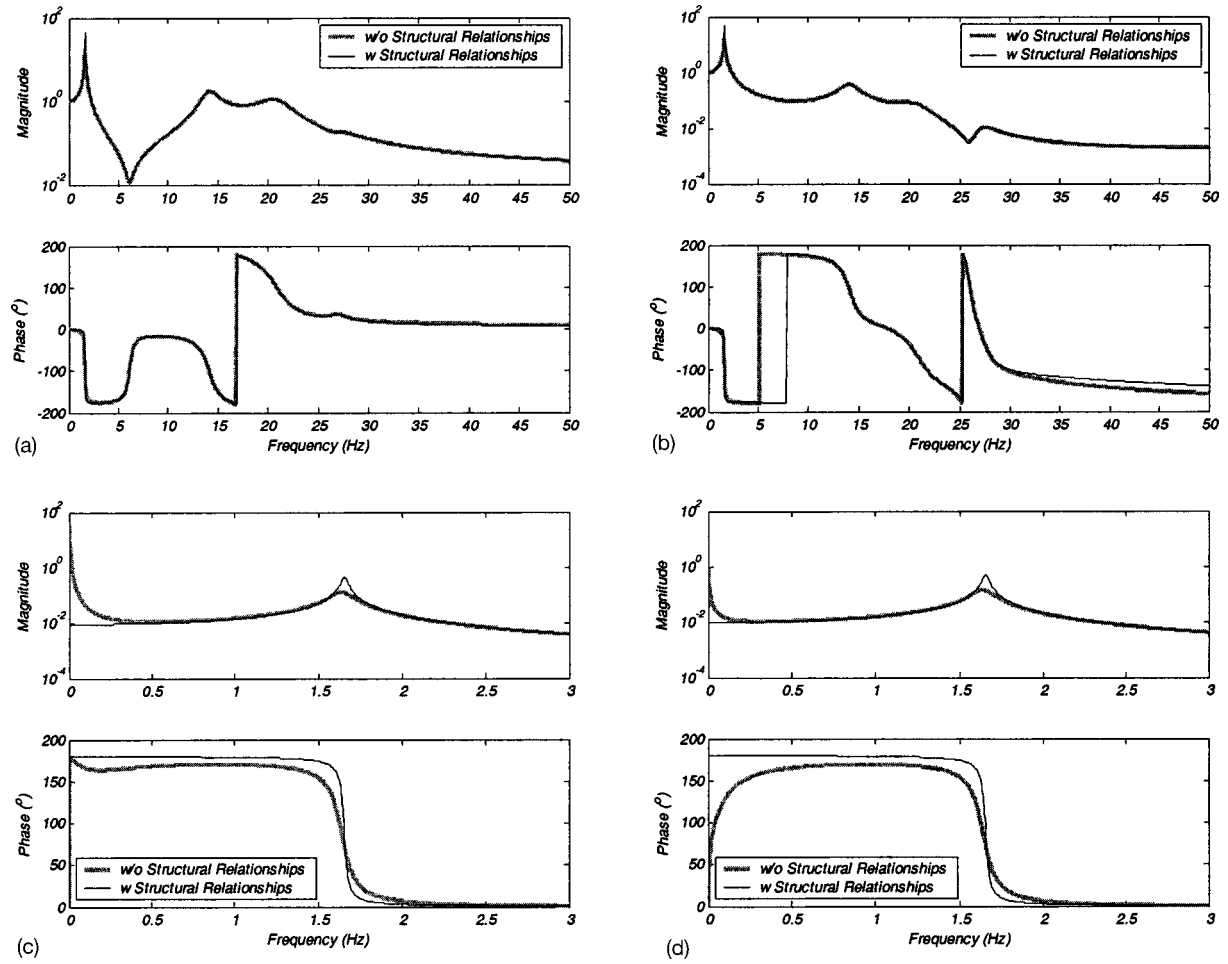

Fig. 9. Comparison of estimated frequency response function (FRF) with respect to inclusion of the physical relationships: (a) FRF or absolute acceleration of foundation base from ground acceleration; (b) FRF for absolute acceleration of superstructure from ground acceleration; (c) FRF for relative displacement of foundation base from ground acceleration; and (d) FRF for relative displacement of superstructure from ground acceleration

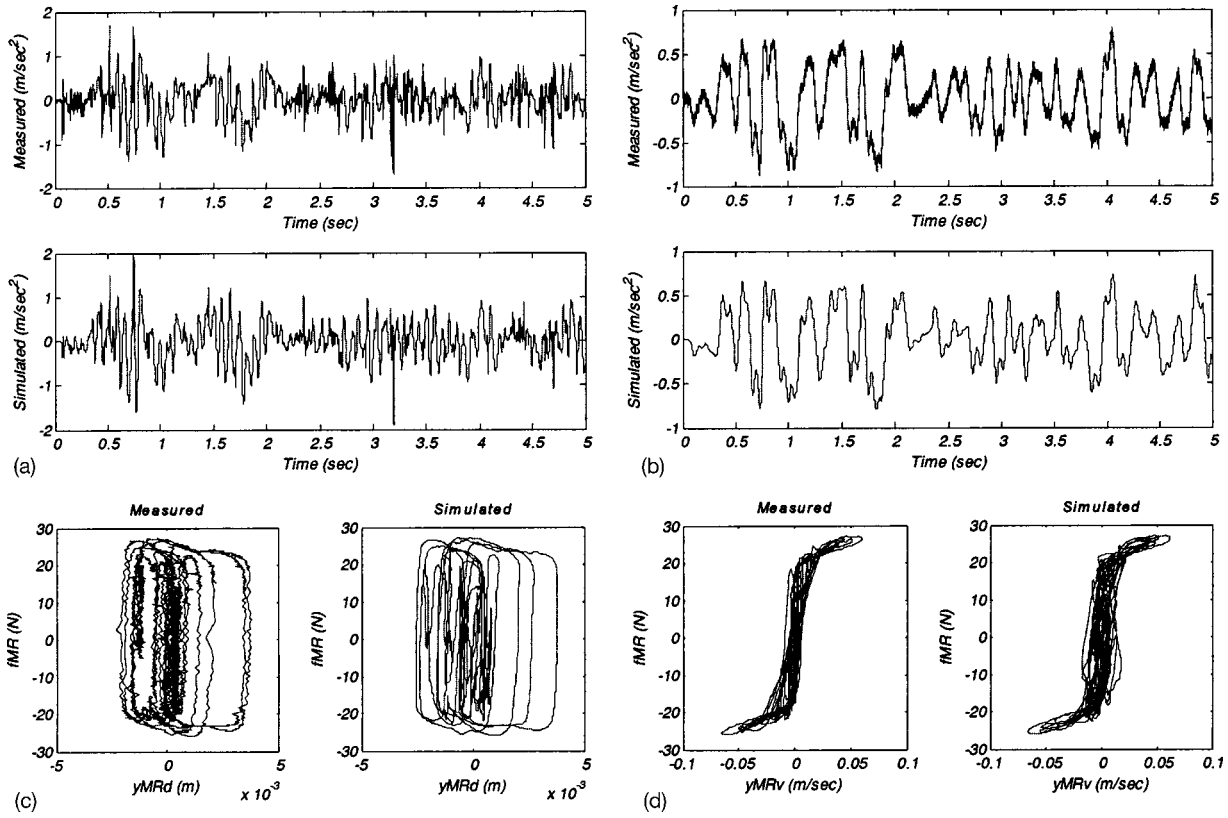

Fig. 10. Time history of measured responses and simulated responses: (a) absolute acceleration of base structure; (b) absolute acceleration of superstructure; (c) displacement hysteresis of magnetorheological (MR) damper; and (d) force-velocity behavior of MR damper

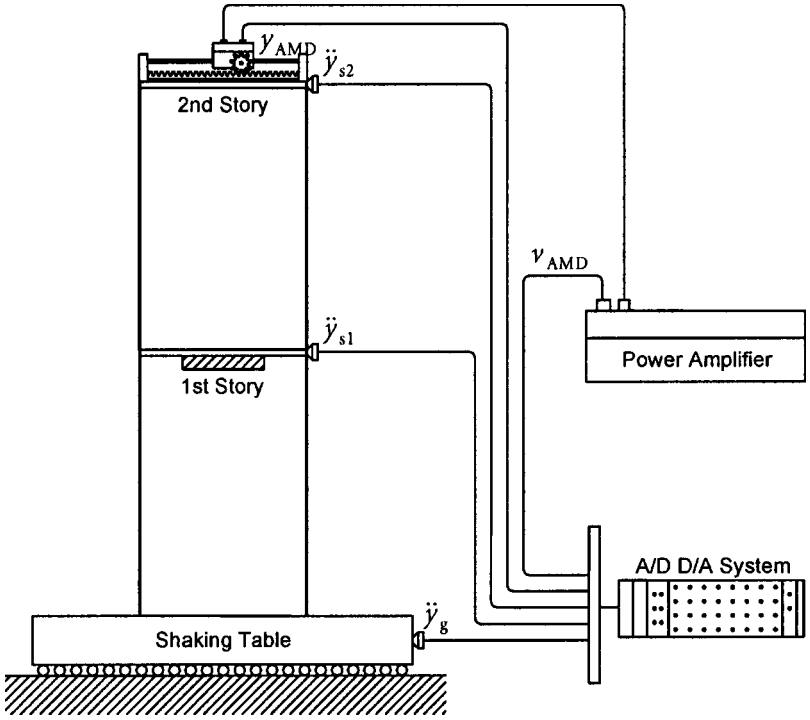

Fig. 11. Experimental setup of the shaking table test at Smart Structures Technology Laboratory

Table 3. Specification of the Seismic Simulator at Smart Structures Technology Laboratory

Aluminum sliding table	46 cm × 46 cm	Maximum displacement	±10 cm
Operational frequency range	0–20 Hz	Maximum velocity	±80 cm/s
Maximum payload	15 kg	Maximum acceleration	±2.5*g*

device (Spencer and Nagarajaiah 2003). To take into account the effects of the MR damper on the structure, not only the measured accelerations but also the unmeasured responses such as relative displacements and relative velocities of the structure with respect to the MR damper should be simulated accurately from the estimated system model (Yoshioka et al. 2002). As shown in Fig. 9, good estimation of the measured acceleration responses does not guarantee the good estimation of such unmeasured relative responses. Figs. 10(c and d) show that the presented method can catch the nonlinear characteristics of the input-output relationship from the MR damper's force to the unmeasured structure's relative responses. Simulation results show that the proposed method can identify the rational polynomial transfer function model of the smart base-isolated structure employing an MR damper quite well.

Table 4. Identified Modal Characteristics of the Bench-Scale Building with Active Mass Driver

Mode number	First	Second	Third
Natural frequency (Hz)	0.927	2.69	19.8
Modal damping ratio (%)	0.951	1.29	54.7

Two-Story, Bench-Scale Building Employing an Active Mass Driver

In this experiment, system identification of a two-story, bench-scale building employing an active mass driver (AMD) is considered (Fig. 11). Shaking table tests are conducted using a uniaxial seismic simulator at the Smart Structures Technology Laboratory (SSTL) at the University of Illinois at Urbana and Champaign ⟨http://cee.uiuc.edu/sstl/⟩. The specifications for the seismic simulator are summarized in Table 3 (Battaini et al. 2000).

The two-story, bench-scale building is constructed using the structural specimen manufactured by Quanser Consulting Inc., so it can be represented by a flexible shear building model. The interstory height is 490 mm, and each column is made of a steel plate with a section of 2×108 mm. The mass of first story is 1.689 kg and the second story mass is 1.662 kg. An AMD is installed on the top floor of the building to reduce the vibration of the building due to the earthquake excitation. It consists of a moving cart with a DC motor that drives the cart along a geared

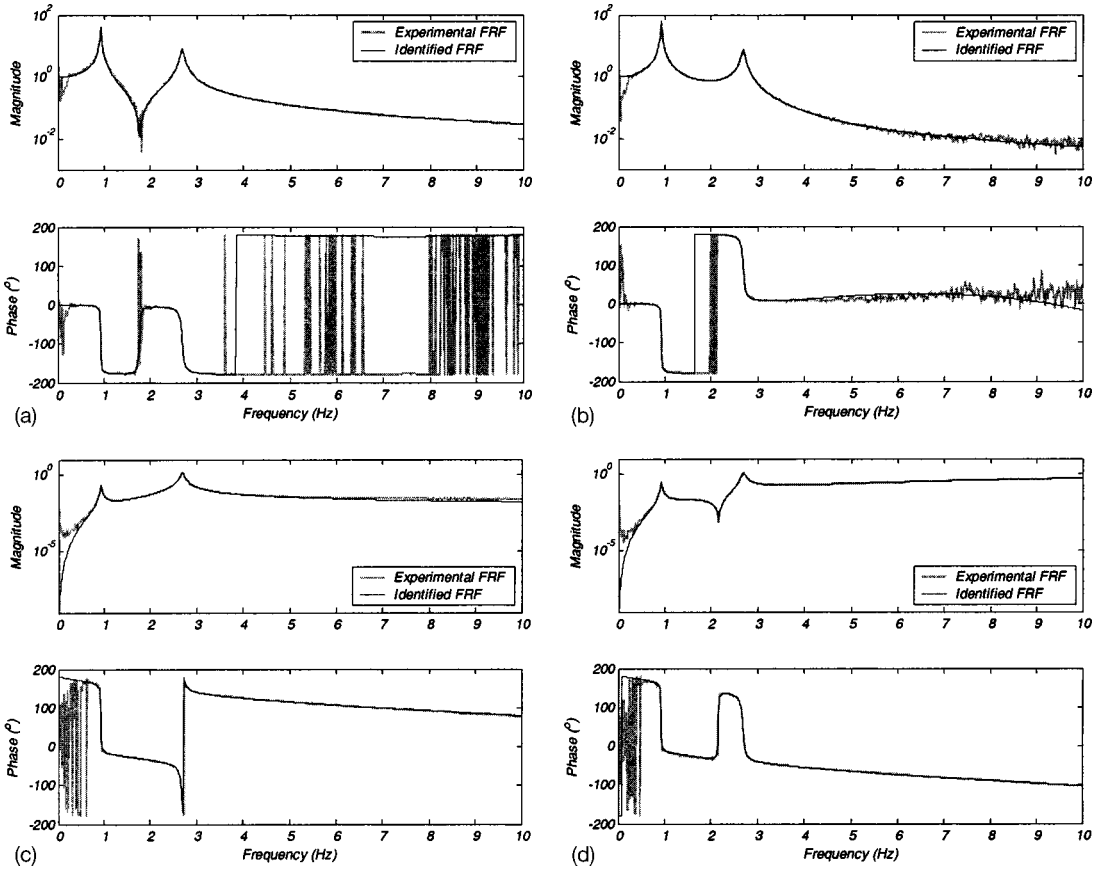

Fig. 12. Identified frequency response functions: (a) frequency response function (FRF) for absolute acceleration for first story from ground acceleration; (b) FRF for absolute acceleration for second story from ground acceleration; (c) FRF of absolute accelerations for first story from active mass driver (AMD) command; and (d) FRF of absolute acceleration for second story from AMD command.

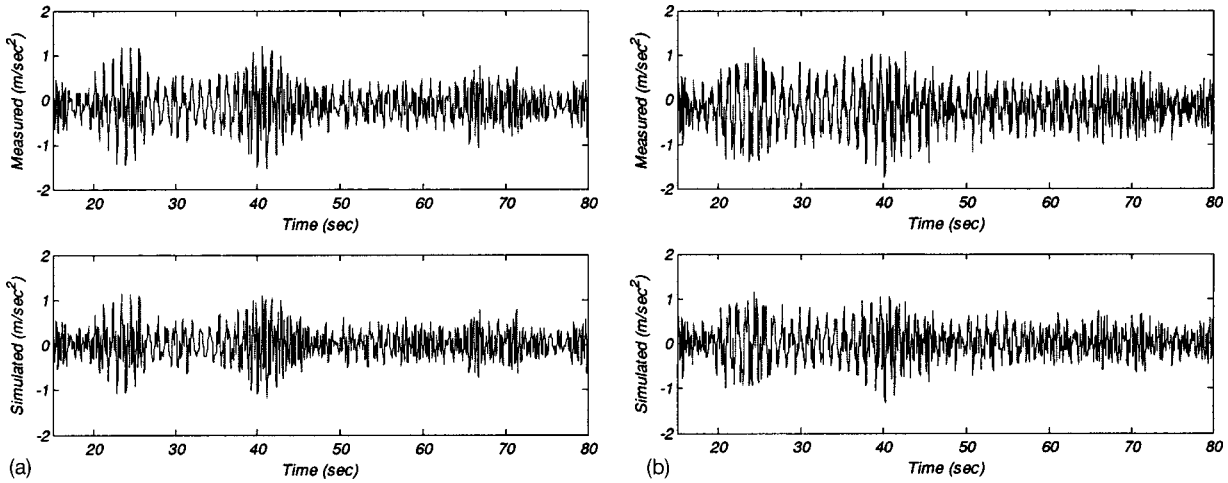

Fig. 13. Time history of measured responses and simulated responses: (a) absolute acceleration of first story; and (b) absolute acceleration of second story

rack. The total moving mass is 454 g and the maximum stroke is ±9.5 cm. The cart is controlled by a PD controller with displacement feedback (Battaini et al. 2000).

In this experiment the system has two inputs, which are the earthquake's ground acceleration and the command signal of the AMD controller. Using the *MFDID* program, a rational polynomial model for the bench-scale building with the active mass driver is identified. The frequency ranges below 0.35 Hz and above 10.0 Hz are excluded to eliminate the DC error and to prevent the unwanted higher mode effects, respectively. The identified modal parameters are summarized in Table 4. The first two modes correspond to the building modes, whereas the third mode is due to the combined dynamics of the AMD and the building. The identified FRF is compared with the experimental FRF data in Fig. 12. The identified model shows good agreement with the experimental FRF data in the frequency range under 10 Hz.

Numerical simulation using the identified model has been conducted to verify the suggested method. Measured signals of the ground acceleration and the control command of AMD are applied to the identified system model, and simulation responses of the system model are compared with measured responses of the structure. The signal-to-error ratios $[20\log(\sigma_{\text{Signal}}/\sigma_{\text{Error}})]$ are found to be 8.88 dB for the absolute acceleration of the first story and 6.90 dB for the absolute acceleration of the second story (Fig. 13).

Simulation results show that the proposed method is quite effective in identifying the system model of the actively controlled bench-scale building.

Concluding Remarks

A frequency domain system identification method has been developed to obtain a rational polynomial transfer function model of MIMO structural systems based on a maximum likelihood approach. Physical relationships between the measured variables are incorporated and a three-stage procedure is deployed. The suggested method has been realized in a graphical user interface program, *MFDID*. Shaking table tests of a smart base-isolated structure employing an MR damper and an actively controlled bench-scale building were conducted to verify the proposed approach and the developed program. FRFs of the identified model and simulated responses of the structure demonstrated that this method is effective and robust for the system identification of MIMO systems.

Acknowledgments

This work was supported in part by a postdoctoral fellowship to the first writer from Korea Science & Engineering Foundation (KOSEF) and by the National Science Foundation under Grant No. CMS 00-00234 (Dr. S. C. Liu, Program Director)

Appendix

Proof of maximum number of zeros of transfer function for relative displacement (Hildebrand 1965).

Let us rewrite Eqs. (3) and (4) by augmenting as follows:

$$H_{y_{sr}u}(s) = [I \quad 0]\Lambda\begin{bmatrix} 0 & 0 \\ M_s^{-1}B_{se} & -B_{sg} \end{bmatrix}$$
$$= [I \quad 0]\begin{bmatrix} \Lambda_{11} & \Lambda_{12} \\ \Lambda_{21} & \Lambda_{22} \end{bmatrix}\begin{bmatrix} 0 & 0 \\ M_s^{-1}B_{se} & -B_{sg} \end{bmatrix}$$
$$= \Lambda_{12}[M_s^{-1}B_{se} \quad -B_{sg}] \tag{19}$$

where $\Lambda = (s\mathbf{I}-\mathbf{A})^{-1} = \text{Adj}(s\mathbf{I}-\mathbf{A})/|s\mathbf{I}-\mathbf{A}|$.

The above equation shows that maximum number of zeros is maximum order of s in the numerator of matrix Λ_{12}. The numerator of Λ is the adjoint marix of $s\mathbf{I}-\mathbf{A}$. The adjoint matrix is the transpose of the cofactor matrix of $s\mathbf{I}-\mathbf{A}$. The cofactor matrix $C_{i,j}$=signed version of a minor of $s\mathbf{I}-\mathbf{A}$, given by

$$C_{i,j} \equiv (-1)^{i+j}M_{i,j} \tag{20}$$

where the minor $M_{i,j}$=reduced determinant of a determinant expansion that is formed by eliminating the ith row and jth column of a matrix. The numerator of the (i,j)th element of Λ_{12} is the $(j+n_s,i)$th element of the signed minor of $s\mathbf{I}-\mathbf{A}$. Every row of the matrix, $s\mathbf{I}-\mathbf{A}$, has only one element which is a first order polynomial equation of s. By eliminating the $j+n_s$th row and ith column of a matrix, $s\mathbf{I}-\mathbf{A}$, the maximum number of zeros can be obtained as $2n_s-2$.

References

Anthonis, J., Swevers, J., Moshou, D., and Ramon, H. (1999). "H^{∞}-controller design for a vibrations isolating platform." *Control Eng. Pract.*, 7, 1333–1341.

Balmès, E. (1996). "Frequency domain identification of structural dynamics using the pole/residue parameterization." *Proc., XIV Int. Modal Analysis Conf. (IMAC)*, Dearborn, 540–546.

Barford, L. (1997). "Frequency domain system identification when assuming unknown but bounded errors." *Hewlett-Packard Report, HPL97-35*, Hewlett-Packard, Cupertino, Calif.

Battaini, M., Yang, G., and Spencer, B. F., Jr. (2000). "Bench-scale experiment for structural control." *J. Eng. Mech.* 126(2), 140–148.

Chae, K. C. (2000). *The chae lectures on statistics*, KAIST, Taejon, Korea.

de Vries, D. K., and Van den Hof, P. M. J. (1998). "Frequency domain identification with generalized orthonormal basis functions." *IEEE Trans. Autom. Control* 43(5), 656–69.

Dennis, J. E., Jr., and Schnabel, R. B. (1983). *Numerical methods for unconstrained optimization and nonlinear equations*, Prentice Hall, Englewood Cliffs, N.J.

Dyke, S., et al. (1994). "Absolute acceleration feedback control strategies for the active mass driver." *Proc., World Conf. on Structural Control*, 2, TP1:51–60.

Ewins, D. J. (1991). *Modal testing: Theory and practice*, Wiley, New York.

Goodwind, G. C., and Sin, K. S. (1984). *Adaptive filtering prediction and control*, Prentice Hall, Englewood Cliffs, N.J.

Hildebrand, F. B. (1965). *Methods of applied mathematics*, Prentice Hall, Englewood Cliffs, N.J.

Hong, K. S., and Yun, C. B. (1993). "Improved method for frequency domain identifications of structures." *Eng. Struct.*, 15(3), 179–188.

Huang, S. Y., and Youcef-Toumi, K. (1999). "Zero dynamics of physical systems from bond graph models—Part I: SISO systems." *J. Dyn. Syst., Meas., Control*, 121(1), 10–17.

Jin, G., Sain, M. K., and Spencer, B. F., Jr. (2000). "Frequency domain identification with fixed zeros: First generation seismic-AMD benchmark." *Proc., American Control Conference*, 981–985.

Juang, J. N. (1994). *Applied system identification*, Prentice Hall, Englewood Cliffs, N.J.

Kumar, P. R., and Varaiya, P. (1986). *Stochastic systems, estimation, identification and adaptive control*, Prentice Hall, Englewood Cliffs, N.J.

Levi, E. C. (1959). "Complex-curve fitting." *IEEE Trans. Autom. Control*, 4, 37–44.

Ljung, L. (1999). *System identification: Theory for the user*, 2nd Ed., Prentice Hall, Englewood Cliffs, N.J.

Luenberger, D. G. (1984). *Linear and nonlinear programming*, Addison-Wesley, Reading, Mass.

Mamum, A. A., Lee, T. H., and Low, T. S. (2002). "Frequency domain identification of transfer function model of a disk drive actuator." *Mechatronics*, 12, 563–574.

McCormack, A. S., and Godfrey, K. R. (1998). "Rule-based auto tuning based on frequency domain identification." *IEEE Trans. Control Syst. Technol.*, 6(1), 43–61.

Oppenheim, A. V., and Schaffer, R. W. (1975). *Digital signal processing*, Prentice Hall, Englewood Cliffs, N.J.

Pintelon, R., Guillaume, P., Rolain, Y., Schoukens, J., and Banhamme, H. (1994). "Parametric identification of transfer function in the frequency domain—A survey." *IEEE Trans. Autom. Control* 39, 2245–2260.

Smith, J. O. (1983). "Techniques for digital filter design and system identification with application to the violin." PhD thesis, Elec. Engineering Dept., Stanford University (CCRMA).

Spencer, B. F., and Nagarajaiah, S. (2003). "State of the art of structural control." *J. Struct. Eng.* 129(7), 845–856.

Yoshioka, H., Ramallo, J. C., and Spencer, B. F., Jr. (2002). " 'Smart' base isolation strategies employing magnetorheological dampers." *J. Eng. Mech.* 128(5), 540–551.

Yun, C. B., and Shinozuka, M. (1980). "Identification of nonlinear structural dynamic systems." *J. Struct. Mech.*, 8(2), 187–203.